

Seismic behavioral fragility curves of concrete cylindrical water tanks for sloshing, cracking, and wall bending

Mohammad Yazdabad^a, Farhad Behnamfar* and Abdolreza K. Samani^b

Department of Civil Engineering, Isfahan University of Technology, Esfahan 8415683111, Iran

(Received January 16, 2017, Revised January 4, 2018, Accepted January 16, 2018)

Abstract. Seismic fragility curves of concrete cylindrical tanks are determined using the finite element method. Vulnerabilities including sloshing of contents, tensile cracking and compression failure of the tank wall due to bending are accounted for. Effects of wall flexibility, fixity at the base, and height-diameter ratio on the response are investigated. Tall, medium and squat tanks are considered. The dynamic analysis is implemented using the horizontal components of consistent earthquakes. The study shows that generally taller tanks are more vulnerable to all of the failure modes considered. Among the modes of failure, the bending capacity of wall was shown to be the critical design parameter.

Keywords: earthquake; concrete cylindrical tank; fragility curve; finite element method; vulnerability

1. Introduction

Experience with the behavior of concrete tanks in past earthquakes confirms the need to produce a reliable tool for seismic design and evaluation of such structures. The fragility curves defined as the spectral acceleration against the probability of exceedance of a certain limit response, like overflow, excessive tensile cracking, and failure under compressive stresses, are known as very effective tools for the same purpose. The Alaska's 1964 earthquake was the first of its kind to result in large scale damages in modern tanks and it initiated the subsequent seismic studies on tanks (Haroun 1980). While the seismic behavior of concrete tanks has been the subject of many studies in the past, developing the fragility curves for various failure modes described as above, has not been focused on as much. As a pioneering study, Jacobsen and Ayre (1951) studied the seismic behavior of rigid wall cylindrical tanks. The first use of digital computers for seismic studies of tanks was done by Edwards (1969). The wall flexibility effect on the hydrodynamic force produced by liquid sloshing in anchored cylindrical tanks was considered in his study. Veletsos and Yang (1977) presented a simplified formula for calculation of natural frequency of a full tank using the Rayleigh-Ritz method. The tank was open at top and was continuously attached to a rigid foundation at base. Tedesco *et al.* (1987) developed an exact analytical method for determining the natural frequencies of a flexible wall cylindrical full tank having height-diameter ratios between

0.1 and 1.5. They concluded that oscillation of the sloshing part of liquid was not influenced by vibration of wall and still liquid. Also, it was insensitive to flexibility of wall. In another study, Tedesco *et al.* (1989) studied the seismic response of different categories of cylindrical tanks being completely or partially full. The hydrodynamic pressure was decomposed into sloshing and still parts. The method was applied to spectrum analysis of those tanks.

Afterwards, Haroun (1980) used the finite elements method to study the seismic behavior of cylindrical tanks. He considered several challenging parameters such as the initial hoop stress due to hydrostatic pressure, coupling of wall and liquid vibrations, and the flexibility of soil. The studied tanks were open topped. Until about 2000, most solution results for liquid sloshing in tanks were based on a rigid wall. Fischer and Rammerstorfer (1999) studied the effects of wall flexibility on liquid sloshing. They presented an analytical method for inclusion of wall flexibility in free board estimation in tanks.

Barrios *et al.* (2007) presented a numerical method for calculation of wave height, base shear and bending moment of cylindrical tanks. They used the finite difference method for solving the nonlinear equations of motion and used the ratio of liquid depth to tank radius as a main geometrical parameter. Amiri and Sabbagh-Yazdi (2012) investigated the influence of dome roofs on the natural frequencies and mode shapes of on-ground tanks. Three tanks with the same height differing in diameter were studied using the finite element method. It was resulted that existence of a dome roof only affects the lateral modes of vibration and is negligible for other modes.

One of the recent studies on dynamic behavior of cylindrical concrete tanks is that of Moslemi and Kianoush (2012). They investigated the effects of wall flexibility, vertical ground acceleration and base fixity on the seismic response of tanks using both time history and free vibration analysis. It was shown that only the fundamental impulsive

*Corresponding author, Ph.D.

E-mail: farhad@cc.iut.ac.ir

^aM.Sc.

E-mail: mohamad.yazdabad@gmail.com

^bPh.D.

E-mail: akabiri@cc.iut.ac.ir

Table 1 Geometrical characteristics of the studied tanks

Tank	Height (m)	Diameter (m)	Wall thickness (m)	Aspect ratio, H/D	Height of liquid (m)
Tall	13	17.3	0.3	0.75	12
Medium	10	20	0.3	0.5	9
Squat	7	25.2	0.3	0.27	6

and convective modes are sufficient for characterizing the dynamic response of such tanks to horizontal excitations. They concluded that the current design procedure for estimating the hydrodynamic pressure of liquid is too conservative.

Moeindarbari *et al.* (2014) investigated the seismic behavior of isolated elevated liquid storage tanks using multi-phase friction bearings through a probabilistic analysis. Multi-phase friction pendulum bearing represents a new generation of adaptive friction isolation system to control super-structure demand in different hazard levels. Seleemah and Sharkawy (2011) conducted a research about isolated elevated liquid storage tanks. In their research the structure with elastomeric or sliding bearings was modeled in SAP2000 software. It was found that base isolation was quite effective in reducing the earthquake response of elevated liquid storage tanks in which high reductions of base shear and shaft displacement were achieved.

Most of the seismic vulnerability studies on tanks have been on steel tanks containing oil and liquid chemical substances. Bhargava *et al.* (2005) evaluated the seismic performance of spherical tanks containing liquids. They estimated the crack width and spacing and quantified the leak rate and the average time of a complete outflow of the liquid. They also presented vulnerability curves as the probabilities of a certain level of damage against the peak ground acceleration (PGA). Berahman and Behnamfar (2009) presented the probabilistic vulnerability curves for steel cylindrical tanks of refineries. They utilized an updated Bayesian approach to evaluate unknown parameters of the demand model for the elephant foot buckling and weld failure at the wall-bottom plate connection.

Regarding the existing need on vulnerability assessment methods and tools for concrete tanks, in this paper fragility curves are presented for cylindrical open topped concrete tanks. Tall, medium, and squat tanks are included. The fragility curves will be given for limiting cases including sloshing of water, and tensile cracking and compression failure of wall in bending. Effects of important parameters such as wall flexibility and connection fixity at the base are also studied.

2. The studied tanks and modeling issues

2.1 Geometrical dimensions

For the purposes of this study, three cylindrical concrete untopped tanks with different height-diameter ratios (HDR's) are selected. Since the concrete tanks are usually built with HDR's between 0.2-0.8, concrete tanks with the

Table 2 Calculated reinforcement in hoop and vertical directions

Tanks	Area of hoop reinforcement for unit width of wall (mm ² /m)	Area of vertical reinforcement for unit width of wall (mm ² /m)
Tall	3825.36	1722
Medium	3456.66	1416
Squat	1887	1019

Table 3 Wall material properties

Type	Poisson's ratio	Elastic modulus (GPa)	Density (kg/m ³)
Concrete	0.16	24.86	2400
Steel	0.3	205	7850

HDR's 0.75, 0.5 and 0.25 are selected. The tanks are designed based on ACI 350.3 (2006) assuming a 90% fill. The volume of liquid is made identical for all of tanks, for the effect of HDR to be able to be identified. For design purposes, the tanks are assumed to be located in a high seismicity area on a firm soil. The wall-base connection is fixed in design and the base is assumed to be rigid. The geometrical characteristics of the studied tanks are presented in Table 1.

The hoop and vertical reinforcements have been calculated for the axial forces and bending moments. Their values are given in Table 2. There is no prestressing.

2.2 Modeling issues

After structural design of tanks, they are modeled in Abaqus 6.11 (2011) for the seismic vulnerability study. The liquid part is modeled using the solid elements (C3D8R) while conventional shell elements (S4R) are used for modeling of the wall. C3D8R is an 8-node linear brick element with a reduced integration capability. S4R element is a 4-node quadrilateral shell element with reduced integration. The reinforcing bars with their diameters, spacings and directions are modeled within the shell elements, comprising homogeneous shell sections within Abaqus. The wall material behavior is considered to be linearly elastic in the analysis. The material properties are mentioned in Table 3.

Use is made of the explicit integration procedure for numerical calculations. Therefore the finite element's mesh dimension and the time step are critical parameters of the analysis. A sensitivity analysis on the mesh dimension resulted in the fact that using too fine a mesh results in divergence of results. Optimizing the liquid's mesh was implemented using a coarser mesh in the central zone where the liquid deformation is small and a finer mesh around the perimeter. The mesh types are hexahedral for the liquid and quadrilateral for the wall. The shapes of these elements are shown in Fig. 1. The time step is automatically selected by the software in order to minimize the sensitivity of analysis to elements dimensions. The finite element mesh of the sample tank is shown in Fig. 1.

At the interface between the liquid and wall, a general normal and tangential behavior is introduced. For the

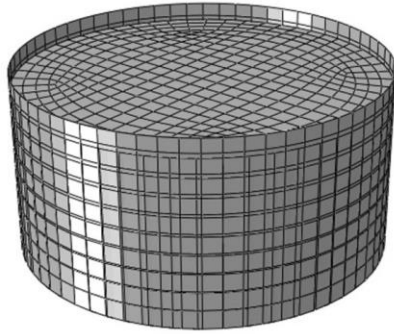


Fig. 1 The finite element mesh of the sample tank.

normal contact, compression is stiff, i.e., the wall and liquid elements cannot overlap, but tension is soft and gap formation is possible. For the tangential contact, slip happens without friction. The liquid (water) part of the system is considered to be incompressible and non-viscous. An effective approach for modeling liquid in explicit algorithms in Abaqus (2011) is use of the Newtonian viscous shear model and the linear state equation. The bulk modulus functions perform as modifiers for the incompressibility constraint of liquid. To avoid an overly stiff response, the internal forces due to the deviatoric response of the material should be kept several orders of magnitude below the forces due to the volumetric response. This can be done by choosing an elastic shear modulus that is several orders of magnitude lower than the bulk modulus, or by choosing a similarly reduced bulk modulus, or by choosing a similarly reduced bulk modulus. Since sloshing of liquid in an untopped tank occurs freely, the bulk modulus can be selected to be 2-3 times less than its real value and the liquid still behaves as an incompressible material.

To neutralize the shear modes that distort the finite elements mesh, the shear viscosity is used as a modifying parameter. Since water is a non-viscous fluid, the shear viscosity of the liquid part of the model should be selected to be a small value. The appropriate shear viscosity can be determined using value of the bulk modulus. In this study, the mass density of water is assumed to be 1000 kg/m^3 and its dynamic viscosity is 0.0013 N.s/m^2 , and the bulk modulus is 2.2 GPa . It is worth noting that dynamic viscosity that is also referred to as absolute viscosity, or just viscosity, is the quantitative expression of a fluid's resistance to flow (shear).

The damping matrix of the system is calculated as a linear combination of mass and stiffness matrices, or the Rayleigh damping, calculated from Eq. (1)

$$[C] = \alpha[M] + \beta[K] \quad (1)$$

In Eq. (1), $[C]$, $[M]$ and $[K]$ are the damping, mass and stiffness matrices, and α and β are constant multipliers dependent on the natural damping ratios and frequencies of the system. The dynamic viscosity incorporated in the liquid part produces a damping for the fluid (Seleemah and Sharkawy 2011). In a recent study by Moslemi and Kianoush (2012), on concrete tanks they used 0.5% and 5% damping ratios for the sloshing (convection) and rigid parts

Table 4 The natural frequencies and periods

Tank	Frequencies, rad/s		Periods, s	
	1st mode	2nd mode	1st mode	2nd mode
Tall	24.34	52	0.25	0.12
Medium	30.9	49.4	0.2	0.127
Squat	34.8	43.9	0.18	0.143

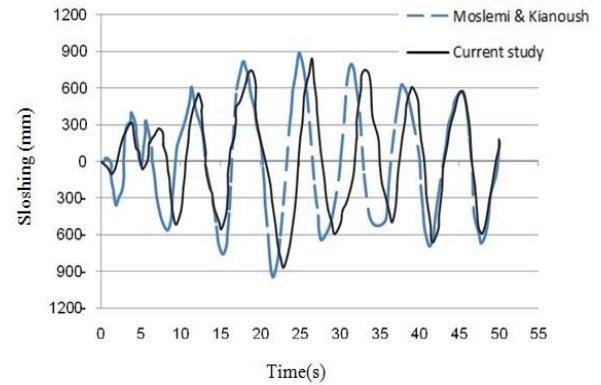


Fig. 2 Sloshing of water surface at the tank wall for the verification study

of the liquid, as recommended by ACI 350.3 (2006).

Since it is not possible in the explicit algorithm of Abaqus to introduce damping for the fluid, damping is defined only for the structure of the tanks and the fluid damping is accommodated by the dynamic viscosity. To calculate the Rayleigh damping coefficient for use in Eq. (1) for the structural part of the system, a free vibration analysis was performed for each empty tank before the dynamic analysis and the natural frequencies were calculated. The first two natural modes having the largest participation factors are called the first and second mode shapes. Their corresponding frequencies and periods are presented in Table 4 for the three studied tanks.

Study on the natural mode shapes and mass participation factors of the empty tanks showed that generally the cantilever modes, i.e., the modes in which the section shape remains circular, have a governing contribution in the tank's vibrational response.

3. Verification analysis

To confirm the validity of modeling assumptions and methodology, a previously studied tank very similar in shape to one of the tanks under study, is selected. This tank was the subject of a recent study on concrete cylindrical tanks by Moslemi and Kianoush (2012). The tank's dimensions are: 12 m in height, 34 m in diameter, and 0.5 m in thickness. The wall-floor connection is fixed and height of fill is 11 m. The dynamic response of the tank has been calculated under the horizontal component of El Centro 1940 scaled to 0.4 g. Sloshing of the water surface at the tank's wall in the plane of loading is selected for comparison. Fig. 2 shows the time histories of sloshing calculated in ref. (Moslemi and Kianoush 2012) and by the current study.

Table 5 Maximum sloshing values at the tall tank's wall in x and y directions under scaled El Centro 1940

Direction of excitation	Maximum sloshing			
	Value (mm)		Time (s)	
	Flexible	Rigid	Flexible	Rigid
x	314	214	29.57	4.94
y	433	348	7.49	42.52

The maximum sloshing levels from ref. (Moslemi and Kianoush 2012) and the current study are 894 and 835 mm according to Fig. 2. Also, the overall trends of the time histories are more or less similar. It is to be noted that because of unavailability of some of the required design data in ref. (Moslemi and Kianoush 2012), certain assumptions have been made when analyzing the same tank in this study. These are not necessarily identical to the original presumptions. Moreover, the Ansys software (Ansys 1997) was used in ref. (Moslemi and Kianoush 2012) for computations whereas Abaqus was made use of in this research. An important difference when analyzing fluids using the above two software is that it is possible in Ansys to introduce an arbitrary damping ratio for the liquid part too but in Abaqus, as practiced in this study, only a dynamic viscosity is possible to assign to the fluid. All of the above factors could have contributed to the observed difference between the results of the two independent calculations in Fig. 2. Despite the above, the comparison seems to be satisfactory and it prepares the ground for the rest of the analysis of this study.

4. Sensitivity analysis on the involving parameters

In this section the relative importance of the main parameters and assumptions is studied before being involved in fragility computations. This will justify inclusion of these factors without which the latter analysis would be implemented with more ease but also with unacceptable inaccuracy. The factors to be studied are wall flexibility/rigidity, base fixity, and height to diameter ratio. The tanks of this study are analyzed in this section concurrently under the perpendicular horizontal components of El Centro 1940 earthquake whose resultant response spectrum is scaled to 0.9 g at the fundamental period of the studied tank. The tanks are assumed to be filled at 90% to arrive at absolutely maximum responses. Although this analysis can be viewed just as an example but yet it shows that true modeling of tanks regarding the studied parameters is important.

4.1 Effect of wall flexibility

The tall tank is selected for the analysis of this section. To simulate a rigid wall, the elastic modulus of the concrete of the wall, E_c , is increased to ten times its actual value. Moslemi and Kianoush (2012) have shown that increasing E_c from $10E_c$ to $20E_c$ does not make a noticeable change in the hydrodynamic pressure of the liquid. Table 5 shows the

Table 6 Maximum hoop force and bending moment in wall of the tall tank under the scaled El Centro 1940, for the flexible and rigid walls

Type of wall	Value		Time (s)	
	Flexible	Rigid	Flexible	Rigid
Hoop force (kN/m)	444.4	265	2.4	2.4
Bending moment (kN.m/m)	84.1	43.4	2.4	2.4

Table 7 Maximum hoop force and bending moment in wall of the tall tank under the scaled El Centro 1940, for the fixed and hinged walls at the base

Base connection	Maximum response			
	Value		Time (s)	
	Fixed	Hinged	Fixed	Hinged
Hoop force (kN/m)	444.4	581	2.4	2.4
Bending moment (kN.m/m)	84.1	23.3	2.4	2.4

values of maximum sloshing at the tank wall at two points in the x and y directions (corresponding to the directions of the horizontal components of earthquake).

According to Table 5, flexibility of wall changes the time and value of the maximum sloshing in both directions considerably. It is responsible for a 46% increase of sloshing in x direction and 24% increase in y direction for the tall tank under El Centro 1940. Table 6 presents the maximum hoop force that occurs at the lower third of wall height. It also shows the peak bending moment about an axis tangent to the mid surface of the wall that happens very near to the base.

As seen in Table 6, ignoring wall flexibility results in a severe underestimation of wall responses. Values of the maximum hoop force and bending moment reduce by 60 % and 51%, respectively, for a rigid wall with respect to the actual flexible wall.

4.2 Level of fixity at the base connection

Connection of wall to its base in concrete tanks can be fixed (clamped) or hinged (free in rotation). The tall tank is again analyzed under the scaled El Centro 1940 with a flexible wall for the fixed and hinged connections at the base. The maximum values of the hoop force and bending moment are calculated. The results are presented in Table 7.

As of Table 7, the hoop force is larger for a hinged wall but the maximum bending moment, which happens at about the midheight, decreases.

4.3 The height-diameter ratio

This part of the sensitivity analysis is implemented to demonstrate that the aspect ratio of a tank is important and different aspect ratios should be taken in response analysis of tanks, similar to the current study.

The aspect ratios considered are the same as what was described in Sec. 2.1, i.e., 0.25, 0.5, and 0.75. As mentioned

Table 8 Maximum hoop force and bending moment in flexible wall tanks fixed at base, under the scaled El Centro 1940

Response component	Maximum response for the tank type		
	Tall	Medium	Squat
Hoop force (kN/m)	444.4	353.9	261.7
Bending moment (kN.m/m)	84.1	44.1	20.41

before, while being different in their aspect ratios, the tanks contain a same volume of water while they are at a 90% of fill. The tanks are modeled with flexible walls fixed at base. Table 8 shows the maximum hoop force and bending moment of tanks wall under the scaled El Centro 1940 earthquake.

Table 8 shows that while the volume of fluid is identical in all cases, the hoop force in the tall tank increases by 25% and 70% with respect to the medium and squat tanks, respectively. Similar values for the bending moment are 90% and 312 % that are too large to be ignored.

5. The seismic fragility curves

5.1 General

A fragility curve generally shows the probability of occurrence of a certain behavior at a specific response parameter. Three types of limit behavior, as observed in past earthquakes, are considered for the tanks in this study. These are overflow of water due to extreme sloshing, a leaking tensile crack in wall due to bending about a horizontal axis tangent to wall surface, and compression failure in wall again due to bending about the latter axis. The calculations are done using elastic dynamic time history analysis with real earthquakes, to be introduced in the next section.

The general method for computing the fragility curves in this study is that each tank is analyzed under each earthquake and the maxima of desired responses are extracted. The analysis is repeated under the same earthquake each time magnified by a certain factor and the magnified responses are calculated. Value of the maximum tensile stress of the vertical bars at the base of the tank wall is used for calculation of the tensile crack width. A Log-Normal probability distribution is assumed for the peak bending moments and crack widths. Then the probabilities of occurrence of a limit crack width enough for leakage as a code prescribed value, and a bending moment equal to or larger than the capacity of wall section, are calculated. As the magnification factor of earthquakes increases, the probabilities are depicted against the spectral acceleration of each tank at its fundamental period, to form the fragility curves. For sloshing, the probability of the sloshing height being larger than the design freeboard is calculated. Specifics of each response parameter are explained in the following.

5.2 The earthquake ground motions and incremental dynamic analysis

Table 9 Characteristics of the selected earthquakes

Record	Earthquake	Station	Date	Magnitude	Larger PGA (g)
NGA0006	Imperial valley	USGS 117 El Centro Array 9	1940-05-19	6.95	0.2584
NGA0322	Coalinga	CDMG 46314 Cantua Creek School	1983-05-02	6.36	0.2806
NGA0832	Landers	CDMG 21081 Amboy	1992-06-28	7.28	0.1298
NGA0752	Loma Prieta	CDMG 47125 Capitola	1989-10-18	6.93	0.4803
NGA0030	Parkfield	CDMG 1014 Cholame - Shandon Array #5	1966-06-28	6.19	0.3768
NGA0950	Northridge	USC 90069 Baldwin Park - N Holly	1994-01-17	6.69	0.1079
NGA0068	Sanfernando	CDMG 24303 LA - Hollywood Stor FF	1971-02-09	6.61	0.2101
NGA1119	Kobe	CUE 99999 Takarazuka	1995-01-16	6.90	0.7069
NGA0138	Tabas	70 Boshrooyeh	1978-09-16	7.35	0.1089

For the purposes of this study, 9 earthquake motions, all recorded on soil Type B (a firm soil, consistent with the design assumption of the tanks) at a far-field distance with magnitudes larger than 6 are selected from the PEER strong motion database. The characteristics of the earthquakes are shown in Table 9.

The purpose is implementing an incremental dynamic analysis under concurrent horizontal components of each earthquake and calculating the maximum responses at equally spaced spectral accelerations. This is carried out as follows. First the response spectrum of each horizontal component of the earthquake is determined. Then a resultant response spectrum is constructed by computing the square root of sum of the squares (SRSS) of the pairs of response spectra of the earthquake. Then the amplitude of the resultant spectrum is set to unity at the fundamental period of the tank. The latter spectrum is then scaled at equally spaced values and the dynamic analysis of the tank is done each time with the earthquake record scaled as above.

In this study, the first scale factor is selected to be 0.3 g and it is increased up to 4.8 g at an increment of 0.3 g resulting totally in 15 increments. This is called an incremental dynamic analysis. The maximum scale factor (4.8 g) is deliberately taken to be so large to make occurrence of the limit responses, described in Sec. 5.1, possible. Therefore, at the end of analysis for each tank, there will be 15 data points available for each response parameter under each earthquake, or $15 \times 9 = 135$ data points for all earthquakes.

5.3 Fragility curves for sloshing

As mentioned before, a freeboard of 1 m has been

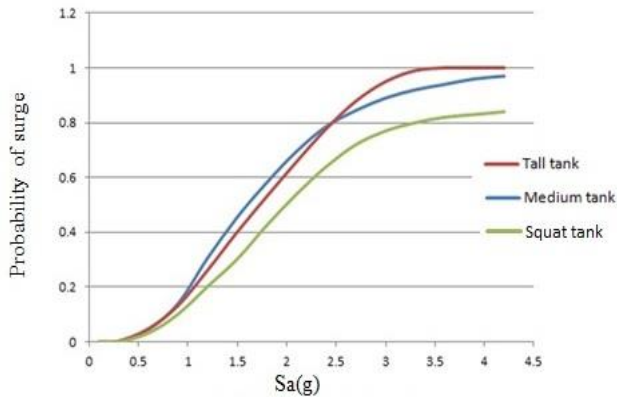


Fig. 3 Fragility curves for sloshing

selected in design of the studied tanks. A fragility curve for sloshing in this study shows the probability of the sloshing wave height to be larger than 1 m for each spectral acceleration value. As explained in Sec. 5.2, there are 135 data points for the sloshing height. Distribution of the data is assumed to be of Log Normal type and the probabilities of them exceeding one meter are calculated. The resulting curves are shown in Fig. 3 for the studied tanks.

It is observed in Fig. 3 that the probability of overflow at each S_a is not much sensitive to the aspect ratio of the tank; it is more related to the value of freeboard itself. Since the volume of liquid is identical for all of the studied tanks, the sloshing height should be a function of the liquid volume, not the aspect ratio. Also, up to very large S_a 's of about 2 g, the probability of overflow hardly exceeds 50% and is not much probable for the cases studied. Therefore, a freeboard of 1 m seems to be appropriate for practical cases.

5.4 Fragility curves for the leaking tensile crack

In this study the fragility curves for a leaking crack show the probability of the crack width exceeding the allowable limit set by ACI 224R-01 (2001), equal to 0.1 mm. For calculation of the crack width, the maximum corresponding bending moment is calculated at each increment of analysis and is converted to the crack width using Eq. (2) (ACI 2005)

$$w_b = 0.011f_s\beta^3\sqrt{d_cA} \times 10^{-3} \quad (2)$$

in which:

w_b =crack width at the surface of wall,

d_c =cover from wall surface to center of nearest layer of steel,

$\beta=(h-c)/(d-c)$ =factor to account for strain gradient (ratio between strain at wall surface and strain at level of reinforcement) in which h is depth of section under bending moment, c is distance between neutral axis and the extreme compression fiber, and d is distance between the extreme compression fiber and the centroid of the main reinforcing steel,

$A=2 d_c S$ =effective area of concrete in tension surrounding the reinforcement, where S is distance between tensile reinforcing bars,

f_s =steel stress.

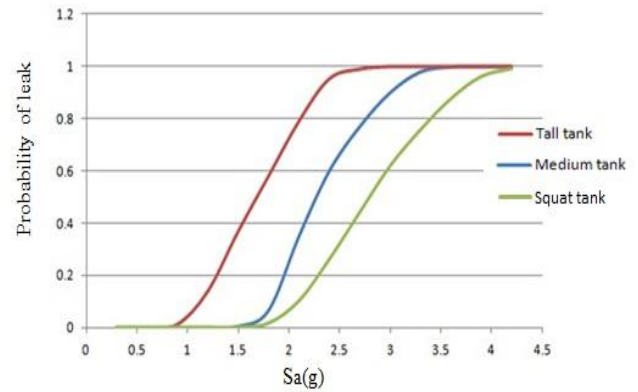


Fig. 4 Fragility curves for the leaking crack width

Value of f_s is a function of the bending moment about the horizontal axis, the vertical normal stress due to the weight of the concrete wall, and the hoop stress, all at the base of the tank wall. Effect of the above parameters has already been included in the current study because a 3D FE model of the tank was analyzed using shell elements. Obviously, interaction of the forces on the vertical and horizontal planes is accounted for in such an analysis. The tensile stress of the vertical bars has been calculated under the combined effects of bending moment and compression force at the horizontal plane at the base of the wall.

The fragility curves of the leaking crack width are shown in Fig. 4.

Fig. 4 shows that probability of growth of a leaking crack is much larger at a certain S_a in taller tanks. For example, at an S_a of 2 g, the mentioned probability is about 80% for the tall tank, while it is only 25% and 5% for medium and squat tanks. This can be attributed to a larger overturning moment in taller tanks because of application of resultant of the hydrodynamic pressure at higher points. On the other hand with the natural periods seen in Table 4 that are also typical to concrete tanks, it is very unlikely for the S_a to be larger than 2 g in any case. Therefore in practical cases only the tall tanks are subject to the risk of developing a leaking tensile crack in strong earthquakes.

5.5 Fragility curves for bending failure of wall

A fragility curve for the wall's bending failure in this research shows the probability of exceeding of the ultimate bending capacity of wall about a horizontal axis tangent to the wall surface, at each S_a . The ultimate bending capacity is determined using the code prescribed formula. In such a calculation, effect of the axial force is disregarded because of its negligible amplitudes in open topped tanks. The fragility curves for bending failure of tank wall are illustrated in Fig. 5.

Fig. 5 shows again that taller tanks are more vulnerable to failure at equal S_a 's. It is while vulnerabilities of the medium and squat tanks against bending failure are very similar to each other. The bending capacity seems to be the critical design parameter of the tank wall as it demonstrates the largest probability of failure at a certain S_a compared with the other two failure modes. For instance, at an S_a of 2

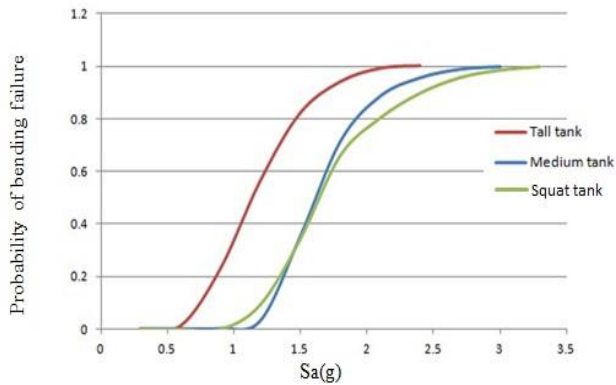


Fig. 5 Fragility curves for wall bending failure

Table 10 Failure probability of the tank wall at $S_a=2$ g for different modes

Failure Mode	Tank type		
	Tall	Medium	Squat
Overflow	38%	39%	32%
Leaking crack	79%	35%	10%
Bending capacity	99%	88%	80%

g, the failure probabilities of the tanks are mentioned in Table 10 based on Figs. 3-5.

Probability of failure of bending capacity is much larger than the other possible failures at such a large spectral acceleration.

6. Conclusions

In this paper fragility curves of water tanks being different mainly in their height-diameter ratio were presented. Three types of tanks being tall, medium and squat regarding their aspect ratio were considered. The tanks were designed according to ACI 350.3 (2006). Then they were modeled using the finite element method and were analyzed utilizing an elastic time history procedure with explicit integration. A verification study confirmed the adequacy of the analysis procedure. Effects of wall flexibility, wall-base connection type, and the aspect ratio were shown to be important for evaluation of seismic behavior of tanks.

For fragility computations 9 consistent earthquakes were selected and an incremental dynamic analysis was performed at equally spaced spectral accelerations. Three different modes of undesired behavior including overflow of the fluid, development of a leaking crack, and bending failure of wall were accounted for. The fragility curves were depicted assuming a Log Normal distribution for the response values. It was shown that generally taller tanks are more vulnerable to all of the failure modes considered. Among the modes of failure the bending capacity of wall was shown to be the critical design parameter.

Comparison of the vulnerability diagrams show that the studied tanks are more vulnerable against failure under wall bending than wall cracking. For instance, in the tall tank, the probability of a critical wall cracking under the spectral

acceleration $S_a=1.8$ g is about 58%. For the same probability, the spectral acceleration is only 1.2 g for the wall's bending failure. Therefore, the wall bending failure is more probable to happen under the same spectral acceleration. The slope of the vulnerability curves is steeper for the tanks having a larger aspect ratio. In other words, for larger spectral accelerations, vulnerability of the taller tanks increases more rapidly than the ones with smaller aspect ratios.

It should be noted that the effect of the vertical components of earthquakes was not discussed in this paper for brevity. In a parallel study by Yazdabad (2013), it has been shown that concurrent application of all three components of earthquake does not change the sloshing height considerably, but increases the bending moment (hence the tensile crack width) for tall, medium and squat tanks by 16, 12 and 6% respectively.

References

- ABAQUS 6.11.1 (2011), Analysis User's Manual, Explicit Dynamic Analysis, Section 6.3.3, Adaptive Meshing, Dassault Systems, MA.
- ACI 318-05 (2005), Building Code Requirements for Structural Concrete and Commentary, American Concrete Institute, Farming Hills, MI.
- ACI Committee 224 (ACI 224 R-01) (2001), Control of Cracking in Concrete Structures, American Concrete Institute, Detroit, Michigan.
- ACI Committee 350.3-06 (2006), Seismic Design of Liquid-Containing Concrete Structures and Commentary, American Concrete Institute, Farmington Hills, MI.
- Amiri, M. and Sabbagh Yazdi, S.R. (2012), "Influence of roof on dynamic characteristics of dome roof tanks partially filled with liquid", *Thin Wall. Struct.*, **50**, 56-67.
- ANSYS (1997), User's Manual, Revision 5.4, ANSYS, Inc., Pennsylvania.
- Barrios, H.H., Zavoni, E.H. and Rodriguez, A.A. (2007), "Nonlinear sloshing response of cylindrical tanks subjected to earthquake ground motion", *Eng. Struct.*, **29**, 3364-3376.
- Berahman, F. and Behnamfar, F. (2009), "Probabilistic seismic demand model and fragility estimates for critical failure modes of un-anchored steel storage tanks in petroleum complexes", *Probab. Eng. Mech.*, **24**, 527-536.
- Edwards, N.W. (1969), "A procedure for dynamic analysis of thin walled cylindrical liquid storage tanks subjected to lateral ground motions", Ph.D. Dissertation, University of Michigan, Ann Arbor, Michigan.
- Fischer, F.D. and Rammerstorfer, F.G. (1999), "A refined analysis of sloshing effects in seismically excited tanks", *Int. J. Press. Ves. Pip.*, **76**, 693-709.
- Haroun, M.A. (1980), "Dynamic Analysis of liquid Storage Tanks", Earthquake Engineering Research Laboratory Report, California Institute of Technology (EERL), Pasadena, California.
- Jacobsen, L.S. and Ayre, R.S. (1951), "Hydrodynamic experiments with rigid cylindrical tanks subjected to transient motions", *Bull. Seismol. Soc. Am.*, **41**, 313-346.
- Kapilesh Bhargava, A.K. and Ghosh, S.R. (2005), "Seismic response and fragility analysis of a water storage structure", *Nucl. Eng. Des.*, **235**, 1481-1501.
- Moeindarbari, H., Malekzadeh, M. and Taghikhany, T. (2014), "Probabilistic analysis of seismically isolated elevated liquid storage tank using multi-phase friction bearing", *Earthq. Struct.*,

- 6(1), 111-125.
- Moslemi, M. and Kianoush, M.R. (2012), "Parametric study on dynamic behavior of cylindrical ground-supported tanks", *Eng. Struct.*, **42**, 214-230.
- Seleemah, A.A. and Sharkawy, M. (2011), "Seismic analysis and modeling of isolated elevated liquid storage tanks", *Earthq. Struct.*, **2**(4), 397-412.
- Tedesco, J.W., Kostem, C. and Kalnins, A. (1987), "Free vibration analysis of cylindrical liquid storage tanks", *Comput. Struct.*, **26**(6), 957-964.
- Tedesco, J.W., Landis, D.W. and Kostem, N.K. (1989), "Seismic analysis of cylindrical liquid storage tanks", *Comput. Struct.*, **32**(5), 1165-1174.
- Veletsos, A.S. and Yang, J.Y. (1977), "Earthquake response of liquid of storage tanks", *Advances in Civil Engineering Through Engineering Mechanics, Proceeding of Annual EMD Specialty Conference*, Rayleigh, N.C.
- Yazdabad, M. (2013), "Development of fragility curves for concrete cylindrical storage tanks", M.Sc. Thesis, Isfahan University of Technology, Esfahan, Iran.

AT